Quantum Cascade Laser Intracavity Absorption Sensor

Andrei Muraviev, Doug Maukonen, Chris Fredricksen, Gautam Medhi, R. E. Peale

Department of Physics, University of Central Florida, Orlando FL 32816

ABSTRACT

A mid-infrared intracavity laser absorption spectrometer based on an external cavity multi-mode quantum cascade laser is combined with a scanning Fabry-Perot interferometer is used as tunable narrow band transmission filter to analyze the laser emission spectrum. Sensitivity as a trace gas detector at 8.1 micron wavelengths has been demonstrated based on a weak water vapor line at an absorption coefficient of 1 x 10^{-5} cm^{-1}. For molecules of reasonably strong absorption cross section (10^{-17} cm^2), this corresponds to a detection limit of 40 ppb.

Keyword list: QCL, sensor, spectrometer, infrared

1. INTRODUCTION

Intracavity Laser Absorption Spectroscopy (ICLAS) is a well-established means of detecting and identifying weak intracavity absorbers [1]. The method involves a multimode laser with an open external cavity that allows introduction of an absorbing sample inside the laser cavity. Since laser gain compensates for cavity losses, the method allows much longer effective path lengths than can be achieved using passive cavity approaches, such as ring-down spectroscopy [2]. This leads to enhanced sensitivity with detection of absorption coefficients as low as 10^{-10}-10^{-11} cm^{-1} [2,3]. The highest optical path achieved was established with a CW dye laser: 70000 km [4].

Since ICLAS was first conceived [5], different gain media have been used. These include Ti:sapphire laser [2], dye lasers [6], color center lasers [7], Nd^{3+} glass lasers [8], diode lasers [9], doped fiber lasers [10], and other solid state lasers. Previous demonstrations have been in the ultraviolet to near infrared wavelength range and in THz [11]. The mid-IR molecular fingerprint region has remained largely unexplored by this technique. There is strong reason to develop a mid-IR ICLAS system, since molecules have characteristic absorption features in the 3 to 12 μm wavelength range. Such a system would have broad application in defense, security, environmental monitoring, medical diagnostics, etc.

Quantum Cascade Lasers (QCLs) are the most promising mid-IR sources for ICLAS [12] due to broadband emission spectra, wide tunability, high output power, high duty cycle, and room temperature operation [13]. The molecular fingerprint region (3-12 μm), where fundamental rotational-vibrational transitions of most molecules lie, is mostly accessible using QCLs, which provide opportunity for constructing portable hand held sensors [14]. Working at the wavelengths corresponding to the vibrational fundamentals gives the highest possible absorption cross sections and improves the sensitivity over sensors based on detection of overtone bands at shorter wavelengths.

Sensing via ICLAS is enabled by operating QCLs in an external cavity. The first external cavity QCL (EC-QCL) was demonstrated in 2001 at cryogenic temperature [17], and since then many groups [15-20] and companies have implemented it. These works have emphasized use of a diffraction grating as external feedback reflector for fine tuning the output spectrum over a dense quasi-continuous longitudinal mode spectrum. In this paper we demonstrate the QCL based ICLAS sensor using an external semiconfocal laser cavity. The achieved effective optical path length of several kilometers, with the laser operating simultaneously over a broad mode spectrum, allows detection of intracavity molecular absorbers with high sensitivity. Preliminary results have been reported in [21-24]. There has been a recent demonstration by another group [25]. The emission spectrum of the laser in the presence of an intracavity absorber is analyzed using a Fabry-Perot (FP) interferometer. With this configuration, we estimate sensitivity to absorption coefficients as small as 1 x 10^{-5} cm^{-1}, which for strongly absorbing molecules corresponds to 40 ppb.

2. EXPERIMENT AND RESULTS

An external cavity quantum cascade laser is formed using an off-axis 90 degree parabolic gold-coated mirror, to collimate the diverging beam from the active crystal, and a plane mirror, which has a small out-coupling hole drilled in its center. The use of a parabolic mirror, as opposed to a collimating lens, minimizes effects of intrinsic reflections and Fabry-Perot resonances on optical interfaces inside the laser cavity.

Temperature stability is very important to the achievable sensitivity, since the QCL spectrum depends strongly on temperature. The temperature of the active medium itself rises rapidly within about 1 ms and stabilizes after about 10 ms, according to our time-dependent measurements of spectral mode structure. This temperature rise is very repeatable pulse to pulse, if the average temperature of the laser mount is stable. We achieve this using a thermoelectric cooler with feedback from thermistors, whose value is monitored with 6 digit precision. The average temperature stability achieved 5-15 minutes after turning on the system is 1 mK.

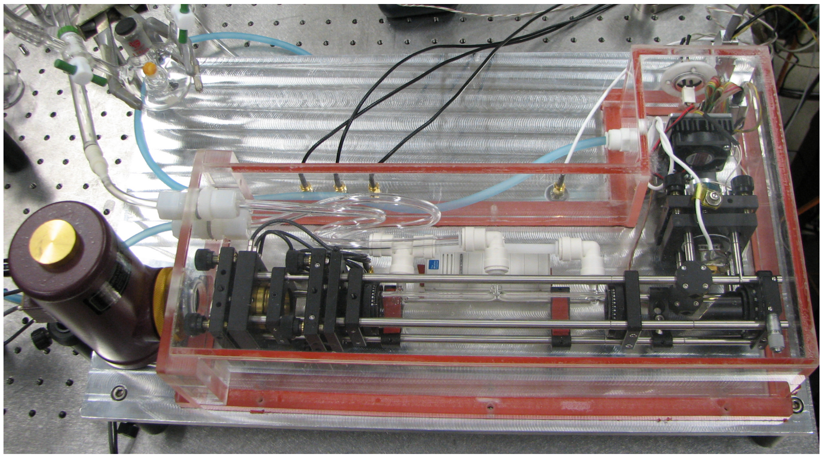

Fig. 1 ICLAS spectrometer in sealed enclosure.

The entire optical system is isolated inside a sealed enclosure that is purged with dry nitrogen (Fig. 1). This eliminates water vapor and other compounds potentially present in ambient air from the laser external cavity. It also provides positive pressure that helps confine the sample within the intracavity gas cell with its open ends.

A gas cell without windows is placed inside the cavity. Sample vapor is prevented from flowing out the ends of the gas cell by balanced flows of sample and nitrogen purge gas. The open ends of the gas cell minimize effects of intrinsic reflections and Fabry-Perot resonances on optical interfaces inside the laser cavity. By diluting a certain volume of pure saturated analyte vapor in dry-nitrogen, we achieve the desired analyte concentration. An automated vapor exchange system allows fast vapor exchange in the gas cell. The exchange of analyte sample and dry-nitrogen reference is synchronized with data acquisition. Vapor exchange rate is 5-10 seconds for the 30 ml volume of the gas cell. Fast spectrum acquisition time combined with this fast vapor exchange rate allows real time monitoring of the analyte-specific absorption. Averaging of spectral measurements for repeated synchronous vapor exchange improves signal-to-noise ratio and enhances overall system sensitivity.

The QCL is driven by 5-10 ms pulses from low-noise current supply. The voltage waveform applied to the QCL is monitoring on an oscilloscope and is used as an indicator for radiation feedback into the active region of the QCL chip, as has been reported in [25]. The resolution and pulse-to-pulse stability of these voltage measurements is hundreds of μV at 600-1000 mA QCL current.

The laser emission spectrum is measured using a scanning Fabry-Perot transmission filter (Fig. 2, left) and 77 K HgCdTe detector at the output of the laser cavity. The intensity transmitted by the Fabry-Perot changes with time during the 10 ms laser pulse due to the spectral changes caused by the aforementioned heating of the active crystal. For each step of the Fabry-Perot mirror, this entire waveform is recorded, acquiring complete time dependence of the QCL spectrum during the pulse. The time resolution of the detector is 1 µs. The Fabry-Perot filter is scanned through its free spectral range, which exceeds the QCL gain bandwidth, by selecting a sufficiently small resonance order for the given finesse. The spectral resolution achieved at the selected resonance order is ~0.5 cm^{-1}. The acquisition time to scan over and collect the full laser emission band at this resolution is 5-60 sec.

The emission spectrum of the system spanned the frequency range 1240 - 1260 cm^{-1} . It is slightly tunable within this range by changing operating current and active chip temperature. Typical spectral dynamics are shown in Fig. 2 (right). The spectrum consists of up to 1 ms continuous fragments followed by jumps to new locations. These jumps are caused by mode hopping due to the thermally expanding laser active element. The mode hopping spectrum behavior along with a continuous drift due to temperature change during the pulse provides continuous coverage of the emission spectral window without gaps.

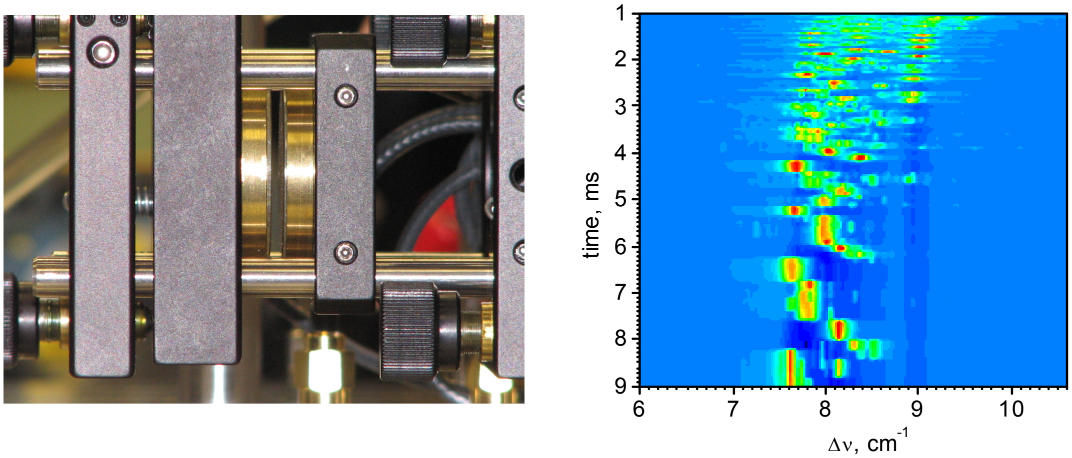

Fig. 2 (left). Piezo tunable FP resonator. (right) Typical time dependence of the laser spectrum measured with FP interferometer. The laser pulse starts at t = 1 ms.

We used water vapor as the first analyte with which to demonstrate the sensing capability. Water a very weak and narrow absorption line [26] in the spectral range of the QCL. We demonstrate two approaches to analyze the spectral data after exposure to this analyte.

The first approach is to monitor one of the continuous spectrum segments between mode hopping events. Fig. 3 presents a fragment of the emission spectrum 140 µs long, taken in the time interval between 2.1 and 2.24 ms from the beginning of the laser pulse. The laser current was 700 mA and the laser average temperature 18 C. Fig. 3 (left) is the reference emission spectrum taken for dry nitrogen in the cavity. Fig. 3 (right) is the emission spectrum when water vapor at 50% humidity level is present inside the gas cell within the cavity. This last spectrum reveals the characteristic sharp absorption line of water vapor. Simultaneously, the presence of the absorption lines broadens the laser spectrum by suppressing mode competition.

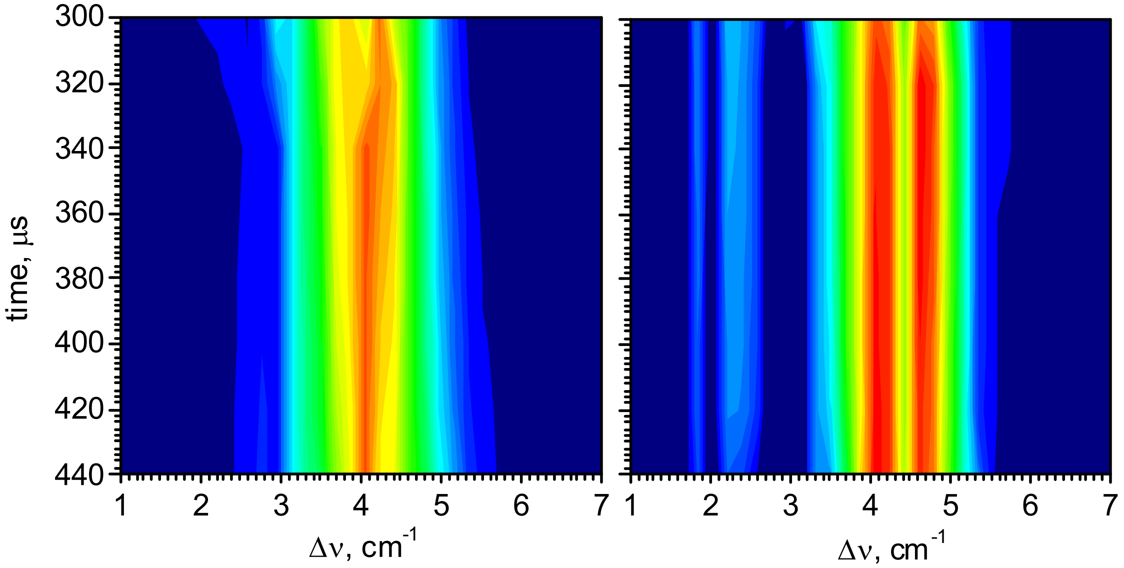

Fig. 3 (left) Fragment of laser spectrum with dry nitrogen inside the gas cell. (right) The same fragment with water vapor in the gas cell. Frequency scale and time scale are relative to the origin point 1.8 ms and 1239.7 cm^{-1}.

Fig. 4(left) presents the time integral of the Fig. 3 from 2.1 to 2.24 ms with calibrated frequency scale and comparison to the reference water absorption spectrum. When water vapor is present, a dip in the laser spectrum clearly coincides with the line in the water spectrum. The broadening of the laser spectrum when water vapor is in the cavity is also clearly demonstrated. Interestingly, the broadened spectrum tends to avoid the position of a second, and even weaker water line at 1242.8 cm^{-1}. This peak has an absorption coefficient of only ~1 x 10^{-5} cm^{-1} and this demonstrates the system sensitivity to be at that level.

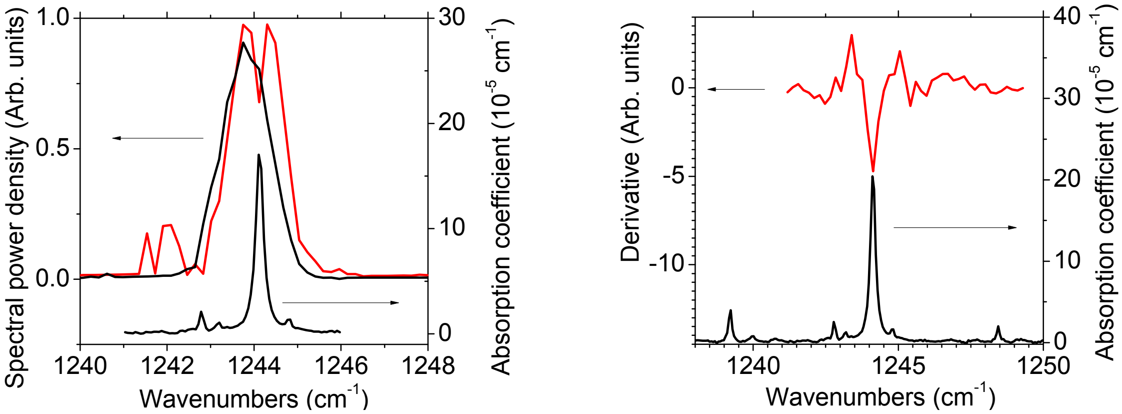

Fig. 4. (left) Laser spectrum integrated in time interval from 2.1 ms to 2.24 ms. Dry nitrogen (black), water vapor (red), together with water vapor reference spectrum [26]. (right) Derivative of the difference spectrum, where the sample spectrum was obtained for nitrogen with ~ 50% humidity and the reference spectrum for dry nitrogen. The Fabry-Perot step size corresponds to a wavenumber interval of 0.18 cm^{-1}, spectral resolution ~0.5 cm^{-1}. The reference absorption spectrum of water vapor, presented in each figure for comparison, was measured at the same ~50% humidity level, so that its absorption coefficient scale applies to our experiment.

The results of the second approach to analyzing the spectral data obtained after the system exposure to water vapor is presented in Fig. 4 (right). This approach is based on the dynamic tuning of the laser through the wavenumber position of the intracavity absorption line. The spectrum was integrated over the entire duration of the pulse (1 to 9 ms), so that all mode hopping events are included. This approach differs from the first by measuring and integrating the effect of the absorber on the dynamics of the mode hopping events. Modes will tend to stay longer at wavenumbers with low absorption and to jump over those wavenumbers where absorption occurs.

Fig. 4 (right) presents the derivative with respect to wavenumber of the difference between the spectra with and without water vapor, because this response function most closely resembles the reference spectrum and is hence easier to interpret. The peak of the derivative represents the fastest drop of the laser spectral power density as the spectrum sweeps across the analyte absorption line. Measurements were performed at an average laser temperature of 18 C. To smooth and broaden the spectrum, data for laser drive currents of 680, 700, and 710 mA were collected and averaged. Each was collected for 5 consecutive vapor exchange cycles. The 700 mA spectrum was measured 3 times, giving a total of 25 vapor exchange cycles. The sharp line on the spectrum derivative precisely matches the position and width of the water vapor absorption line at 1242.12 cm^{-1} on the reference spectrum. The signal-to-noise ratio is approximately 10, which suggests a sensitivity to absorption coefficients at the level of 2×10^{-5} cm^{-1}. A dip appears also at the 1242.8 cm^{-1} position of the weak absorption satellite with a signal-to-noise ratio of about unity, which supports an absorption coefficient sensitivity level of order 10^{-5} cm^{-1}. Considering gases with a reasonably strong absorption cross section of 10^{-17} cm^2 (that of CO^2 near 4.5 microns wavelength peaks at 1.4×10^{-17} cm^2 according [26]), means sensitivity to a concentration of 10^{12} cm^{-3}, or 40 ppb mixing ratio compared with the atmosphere at standard conditions.

3. CONCLUSION

We have measured the sensitivity of the system to sharp-line absorber, where the emission band width of the QCL significantly exceeds the absorption line width. Sensitivity to water vapor, in terms of absorption coefficient, was determined to be about 1×10^{-5} cm^{-1}.

ACKNOWLEDGMENTS

This project was supported by Army Phase I and II SBIRs (Dr. Dwight Woolard PM).

REFERENCES

1. V.M Baev, T. Latz, P.E. Toschek, “Laser Intracavity absorption spectroscopy”, Applied Physics B 69, 171-202 (1999).
2. A. Kachanov, A. Charvat, F. Stoeckel, “Intracavity laser spectroscopy with vibronic solid-state lasers: I. Spectro-temporal transient behaviour of a Ti:sapphire laser”, J. Opt. Soc. Am. B 11, 2412-2421 (1994).
3. A. Garnache, A.A Kachanov, F. Stoeckel, “High-sensitivity intracavity laser absorption spectroscopy with vertical-external-cavity surface-emitting semiconductor lasers”, Optics Letters, 24, 826-828 (1999).
4. J. Sierks, T. Latz, V.M. Baev, P.E. Toschek, “Spectral dynamics of multi-mode dye lasers and single atom absorption”, in Intl. Quantum Electronics Conf., OSA Technical Digest Series (Optical Society of America, Washington DC, 1996).
5. L.N. Pakhomycheva, E.A. Sviridenkov, A.F. Suchkov, L.V. Titova, S.S. Churilov, “Line Structure of Generation Spectra of Lasers with Inhomogeneous Broadening of the Amplification Line”, J. Experimental and Theoretical Physics Lett. 12, 43-45 (1970).
6. T.W. Hänsch, A.L. Schawlow, P.E. Toschek, “Ultrasensitive response of a cw dye laser to selective extinction”, IEEE J. Quantum Electronics QE-8, 802-804 (1972).
7. V.M. Baev, H. Schröder, P.E. Toschek, “LiF:F2+-Center Laser for Intracavity Spectroscopy", Opt. Commun. 36, 57-62 (1981).
8. A.D. Bykov, V.P. Lopasov, Yu.S. Makushkin, L.N. Sinitsa, O.N. Ulenikov, V.E. Zuev, “Rotation-vibration spectra of deuterated water vapor in the 9160-9390-cm-1 region”, J. Mol. Spectrosc. 94, 1-27 (1982).
9. V.M. Baev, J. Eschner, E. Paeth, R. Schuler, P.E. Toschek, “Intra-cavity spectroscopy with diode lasers”, Appl. Phys. B 55, 463-477 (1992).
10. R. Böhm, A. Stephani, V.M. Baev, P.E. Toschek, “Intracavity absorption spectroscopy with a Nd3+-doped fiber laser”, Opt. Lett. 18, 1955-1957 (1993).
11. E. W. Nelson, S. H. Withers, A. V. Muravjov, R. C. Strijbos, R. E. Peale, S. G. Pavlov, V. N. Shastin, and C. J. Fredricksen, “High-resolution study of composite cavity effects for p-Ge lasers,” IEEE J. Quantum Electronics 37, 1525-1530 (2001).
12. J. Faist, F. Capasso, D. L. Sivco, C. Sirtori, A. L. Hutchinson, A. Y. Cho, ‘Quantum Cascade Laser’, Science, 264, 553-556 (1994)

13. Qing Wen and Kirk H. Michaelian, “Mid-infrared photoaccustic spectroscopy of solids using an external cavity quantum-cascade-laser”, Optics Lett., 33, 1875-1877, (2008)
14. A.A. Kosterev, R.F. Curl, F.K. Tittel, M. Rochat, M. Beck, D. Hofstetter, J. Faist, “Chemical sensing with pulsed QC-DFB lasers operating at 15.6 μm”, Applied Physics B: Lasers and Optics 75, 351-357, 2002
15. Andrea Karpf and Gottipaty N. Rao, “Absorption and wavelength modulation spectroscopy of NO2 using a tunable, external cavity continuous wave quantum cascade laser”, Applied Optics, 48, 408-413, (2009).
16. G. P. Luo, C. Peng, H. Q. Le, and S. S. Pei, “Grating-tuned external-cavity quantum-cascade semiconductor lasers”, Applied Physics Letters, 78, 2834-2836 (2001).
17. G. Totschnig, F. Winter, V. Pustogov, J. Faist and A. Muller,” Mid-infrared external-cavity quantum cascade laser”, Opt. Lett. 27 1788–90 (2002)
18. Luo G P, Peng C, Lee H Q, Pei S S, Lee H, Hwang W Y, Ishaug B and Zheng J “Broadly wavelength-tunable external cavity mid-infrared quantum cascade lasers”, IEEE J. Quantum Electron. 38 486–94 (2002)
19. Maulini R, Beck M, Faist J and Gini E , “Broadband tuning of external cavity bound-to-continuum quantum-cascade lasers”, Appl. Phys. Lett. 84 1659–61(2004)
20. T. Tsai, G. Wysocki. “Fast wavelength tuning of external cavity quantum cascade lasers,” Lasers and Electro-Optics, 2009 and 2009 Conference on Quantum electronics and Laser Science Conference. CLEO/QELS (2009)
21. G. Medhi, A. V. Muravjov, H. Saxena, J. W. Cleary, C. J. Fredricksen, R. E. Peale, O. Edwards, Infrared Intracavity Laser Absorption Spectrometer, Proc. SPIE 7680, 24 (2010).
22. G. Medhi, A. V. Muraviev, H. Saxena, J.W. Cleary, C. J. Fredricksen, R.E. Peale, and O. Edwards, Infrared intracavity laser absorption spectrometer, in Proc. Intl. Symp. Spectral Sensing Research, Springfield, Missouri June 21-24, 2010
23. G. Medhi, A.V. Muravjov, H. Saxena, C.J. Fredricksen, T. Brusentsova, R.E. Peale, O. Edwards, “Intracavity laser absoption spectroscopy using mid-IR quantum cascade laser”, Proc. SPIE 8032, 12-19 (2011)
24. Gautam Medhi, Chris J. Fredricksen, Robert E. Peale, Andrey V. Muravjov, Oliver J. Edwards, Sensitivity of long-wave infrared intracavity laser absorption vapor detector, Proc. SPIE 8236 - 55 (2012).
25. Phillips and Taubman, "Intracavity sensing via compliance voltage in an external cavity quantum cascade laser," Optics Letters 37, 2664 (2012).
26. PNNL web data base